Alex. Eng. J., Alex. Univ., Volume 29 No.1 , PP A 41 - A 61 (1990)

SUBCRITICAL CRACK PROPAGATION UNDER CYCLIC SHOCK LOADING

A.I. Gomma, A.H. Hamdy* and Abdelsamie Moet**

* Department of Mechanical Engineering

Faculty of Engineering, Alexandria University

** Department of Macromolecular Science

Case Western Reserve University

Cleveland, OH 44106

Abstract

An equipment has been designed to observe subcritical crack propagation under cyclic shock (impact) loads. The equipment design uses the concept of wave propagation in bars (Hopkinson's bar). A four point bend notched specimen is struck by an incident bar with a known stress wave. The test specimens were machined from PMMA sheet (Lucite) The crack, initiated from the notch, was detected by a step wise increase of a graphitic grid imprinted on one side of the specimen. The data was analyzed using fracture mechanics theory and compared with that of conventional fatigue.

Although the applied strain rate was quite high ($\sim$ 1 s^{-1}), stable crack propagation was significant. It appears that the elastic energy stored in the specimen within the duration of each impact is dissipated in craze formation at the tip of the advancing crack. Furthermore, the magnitude of stable crack propagation was larger under impact loading than under fatigue. On the other hand, cracks were slower under impact loading. Fractographic evidence attributes these phenomena to the nature of craze growth under each loading condition.

1. Introduction

Engineering materials used in the design of moving components have to endure repeated shock loads resulting from clearances existing in machine elements and due to machine functions. It is therefore essential to parameterize the material's endurance under cyclic shock waves as a prerequisite for judicious material usage. Regrettably, present impact tests do not address this important design requirement.

Izod and Charpy test results are inapplicable in material qualification for use under repeated shock loading since both tests employ a single pendulum strike to cause uncontrolled crack propagation. A critical stress intensity factor [1] or a critical energy release rate [2] may be computed from such tests. However, these parameters have no direct significance to cyclic shock wave effects. Furthermore, it should be noted that this type of testing provides a measure of the material's resistance to dynamic crack propagation due to excessive impact overloads. Likewise, repeated impact due to a falling rod [see for example 3] does not produce a well defined shock wave upon load application.

Moreover, conventional fatigue behavior is impertinent, in view of the obvious difference in the loading and unloading patterns. Consequently the need for a testing proceedure to assess the resistance of materials to repeated shock loads is clear. The desired test ought to employ a well defined shock wave in a cyclic fashion. The test results should preferably be presented within a fracture mechanics framework.

This paper desirbes a test apperatus that uses the Hopkinson's bar technique, and demonstrates its utility in observing stable crack

propagation in notched PMMA specimens. The study shows that the crack propagation behavior under impact loading is distinctly different from that under conventional fatigue. It also shows that the critical stress intensity factor associated with shock and fatigue loading is much higher than that observed under a single shock wave [4].

2. Experimental Techniques

A schematic of the testing apparatus is shown in Fig. 1. The design is founded on the principle of stress wave propagation in bars, i.e., the Hopkinson's bar technique [4,5]. A 1420 RPM drive motor (1) strikes the incident bar (10) through an eccentric connecting rod (8) attached to a fly wheel (7). This mechanism generates a compressive stress pulse at the hammer tip (11) which is attached to the far end of the incident bar. The hammer rests completely free to ensure constancy of the shock load. A corresponding bending stress wave passes through the specimen (2) which is supported by a four point bending jig (19). The stress pulse transmited through the specimen is sensed by a force transducer (20) and is recorded on a digitized storage oscilloscope by means of a Whinston bridge (13)/ strain gage (4) system. The number of stress shocks applied is displayed on a digital counter (2).

To generate sinusoidal fatigue cycles a rubber strip of an appropriate thickness is placed between the hammer tip (11) and the free end of the transmitting bar (9). Typical traces of an impact cycle and that of a fatigue cycle are shown in Figs. 2A and 2B, respectively.

The specimen is machined from PMMA (Lucite-L^{R}) sheet to the dimensions shown in Fig. 3. A saw cut is introduced into one edge of the specimen for a depth of about 4 mm. The root of the saw cut was

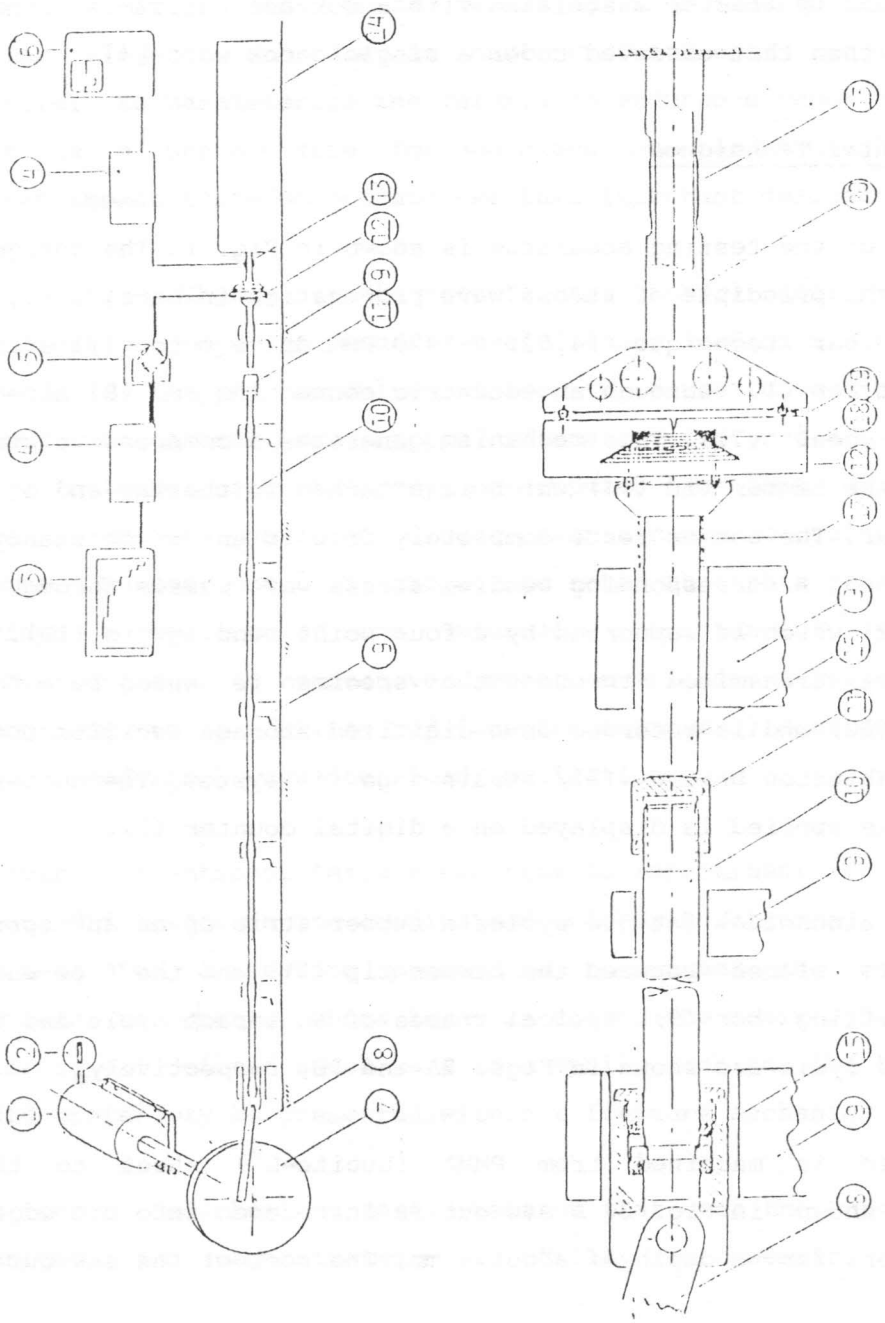

Fig. 1: A schematic illustration of the cyclic shock/fatigue apparatus (top) and a close-up of the specimen jig.

sharpened gently by tapping a razor blade for another millimeter. Crzing was visually observed at the tip of the notch upon introducing the razor. An electrically enductive graphite grid of equispaced lines (18) was imprinted on one side of the specimen adjacent to the notch tip. A Whinston bridge assembly (5) was employed to measure step-wise increase in the electric resistance of the grid due to the passage of the propagating crack. A chart recorder (3) traces the resulting signal as a function of time. The average crack speed is computed from this record.

Tests were designed to examine the effect of the maximum impact (shock) load on the crack propagation behavior and to compare it with equivalent fatigue loads.

The fracture surfaces of the tested specimens were examined by reflected light and scanning electron microscopes to characterize the fracture mechanisms. The exact design of the notch and the transition from quasistatic to dynamic crack propagation were also determined from microscopic examination.

3. Results and Discussions

Considering the transmitted stress wave displayed in Fig. 2A, it is noted that the stress rises to its maximum in a time interval of a little over a mllisecond. Accordingly, the strain rate is in the neighborhood of $1s^{-1}$ suggesting that the applied stress pulse is well within the impact range [7]. The vibrational noise imposed on the load signal in Fig. 2A is attributed to the mass of the bending jig attached to the force transducer.

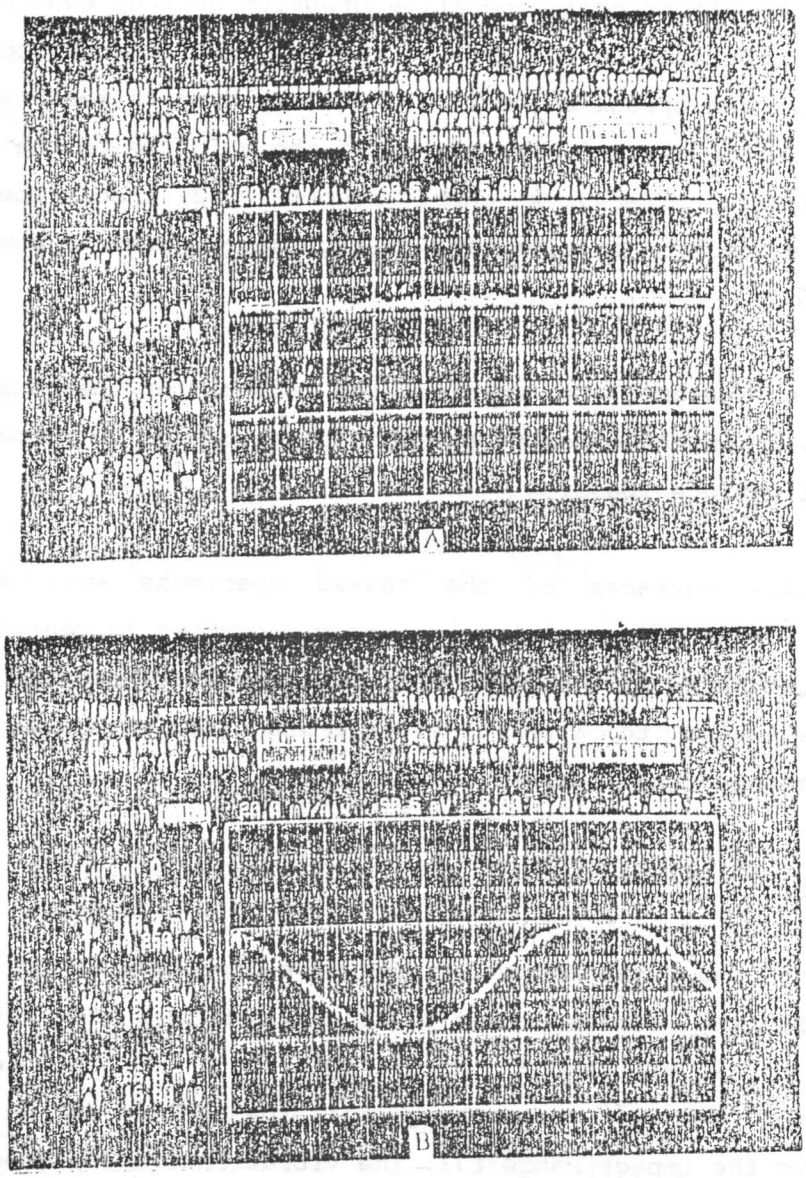

Fig. 2: Typical oscilloscope traces of an shock loading cycle (top) and a fatigue loading cycle (bottom).

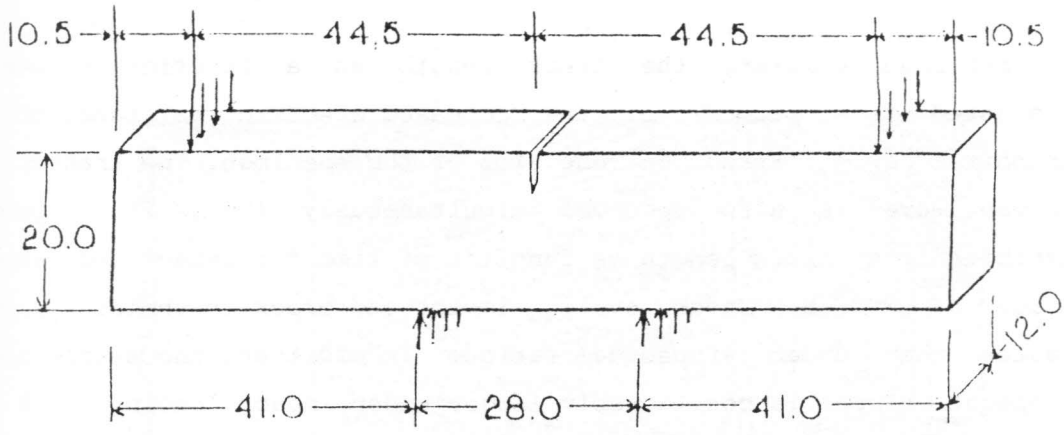

Fig. 3: Specimen geometry and loading configuration. Dimensions are in millimeters.

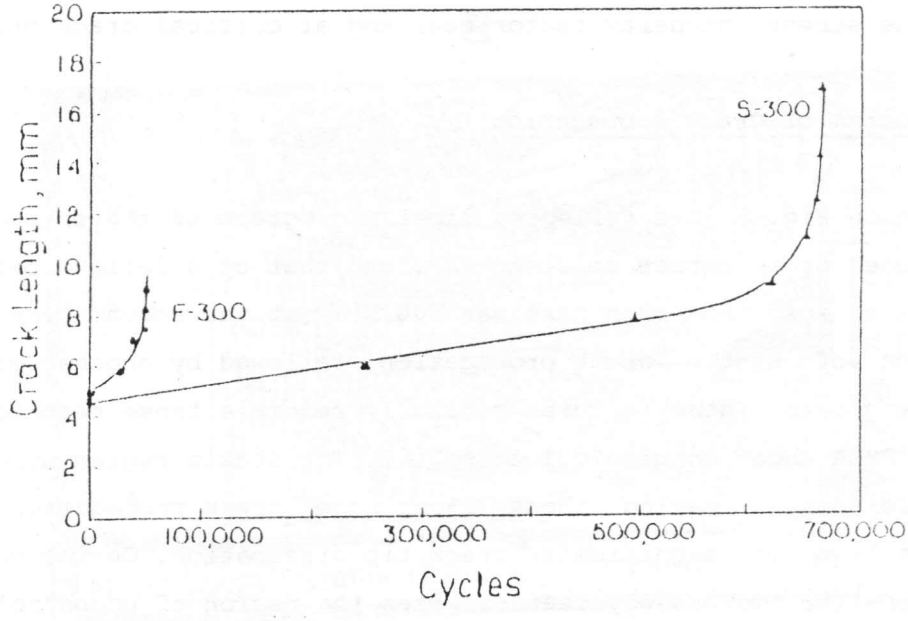

Fig. 4: Crack length vs. number of cycle shock (S—300) and fatigue (F—300) of identical PMMA specimens tested at a maximum load of 300 N.

Crack Propagation Behavior

As outlined earlier, the crack length as a function of time is evaluated from records of the increased electric resistance of the graphitic grid marked on one side of the specimen. The transmitted stress wave is also recorded simultaneously (Fig. 2). Figure 4 exhibits the crack length as function of time for impact and fatigue loads of 300 N. Under cyclic impact the crack is unmistakly much faster than under sinusoidal fatigue. In addition, the stable crack propagation span is considerably longer under impact loading (16.9 mm) than under fatigue (9.1 mm). Consequently, the maximum stress level transmitted through the specimen remains unchanged during the short span of fatigue crack propagation. In the mean time, a small reduction is noted during impact crack propagation as the crack approaches its critical depth. This effect was considered in subsequent calculations of the stress intensity factor near and at critical crack propagation.

Mechanism of Crack Propagation

Shown in Fig. 5 is a reflected light micrograph of the entire fracture surface of an impact specimen (A), and that of a fatigue one (B). The maximum load in each case was 300 N. Past the notch there appears a region of stable crack propagation, followed by another of unstable crack growth. These features generally resemble those reported earlier for PMMA under monotonic loading [8]. The stable region appears rough and displays tearing marks along the crack propagation direction indicative of significant crack tip dissipation. On the contrary, a mirror-like morphology characterizes the region of uncontrolled crack propagation. Besides, discontinuous dynamic crack propagation bands are apparent. None of these features, however, appear when the

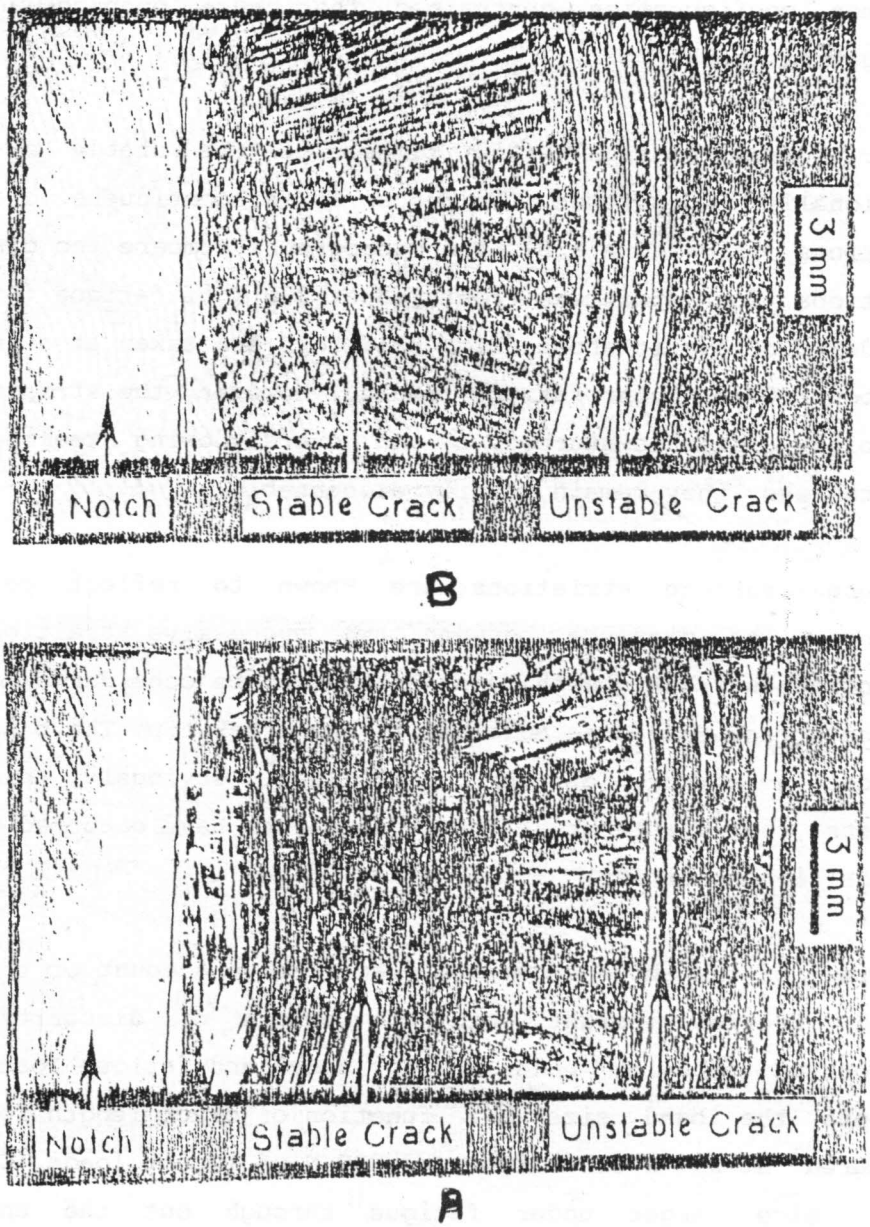

Fig. 5: Reflected light micrographs (5X) of specimens fractured under cyclic shock loading (A) and under fatigue loading (B) of 300 N. Past the notch, the micrographs exhibit the fracture morphologies associated with stable and unstable crack propagation.

fracture surface are examined by the scanning electron microscope. It implies that the height of the remaining crase ligaments is very shallow. Perhaps, this is due to the small imposed load and the specimen configuration contrained the craze opening ahead of the propagating crack.

Higher magnification (250 times) of the stable crack region additionally discloses evidence of discontinuous crack growth striations (Figs. 6 A & B). The micrographs compare the discontinuous striations for specimens fractured at 300 N of fatigue (Fig. 6A) and at 400 N of cyclic shock (Fig. 6B). Both are taken at a crack length of about 10 mm. Under fatigue loading, however, the striated fracture morphology is disturbed by an overshadowing tearing effects. Nevertheless, they remain readily discernable.

Fracture surface striations are known to reflect crack arrest markings. The distance between two successive straition defines a discontinuous crack growth band. A band may be considered as a measure of the crase zone size adjacent to the crack tip. The band size also provides a measure of the crack leap. Obviously, this mechanism suggests that stable crack growth appear to have occurred as a series of local instabilities.

In view of the above argument, quantitative account of the band size should provide insight into the origin of disparity in crack propagation behavior under similar shock and fatigue loads. Figure 7 presents the band size as a function of crack length for specimens fractured at 300 N of fatigue and 300 N of impact loads. Clearly, the band size larger under fatigue through out the entire crack propagation. The deference in the band size becomes progressively

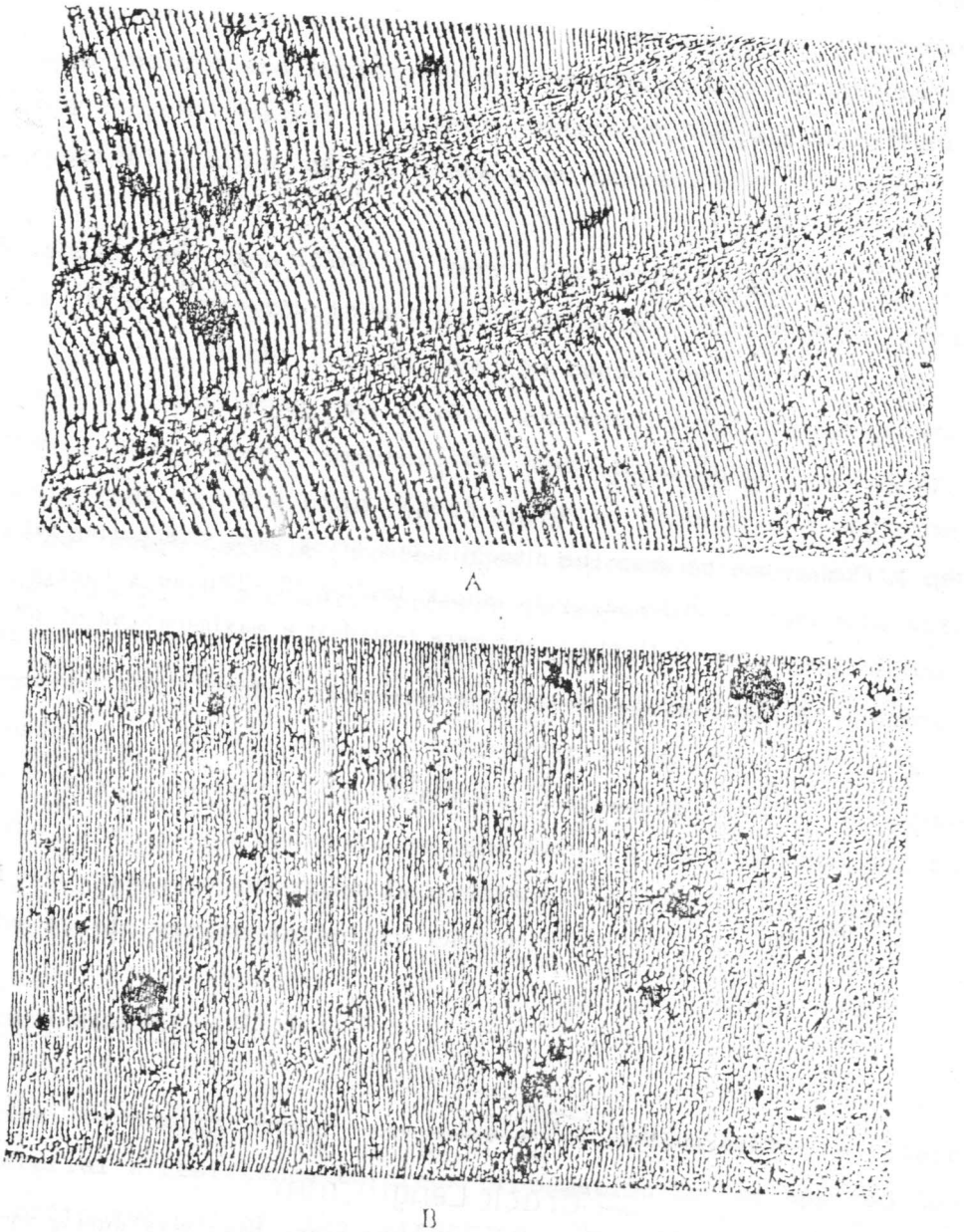

A

B

Fig. 6: Discontinuous crack growth bands in a fatigue specimen fractured at 300 N (A) compared to those in a shock specimens fractured at 400 N. The micrographs (250X) are taken at a crack length of 8 mm in both specimens.

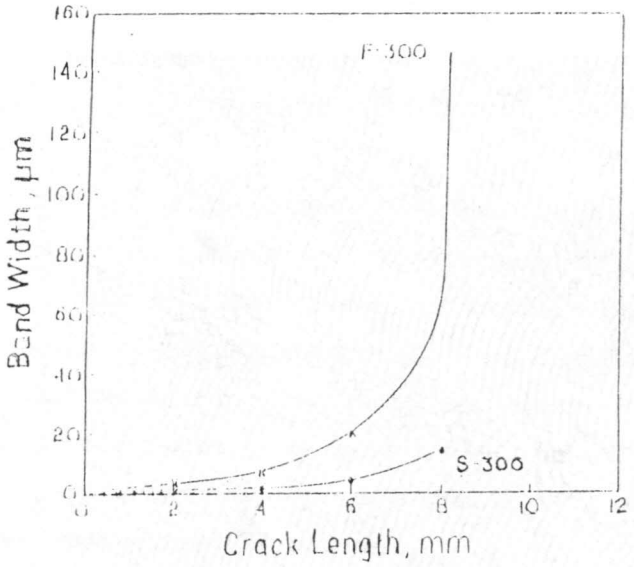

Fig. 7: Comparison between the discontinuous crack band size during fatigue loading (F—300) and cyclic shock loading (S—300) as a function of crack length. Both specimens were tested at a maximum load of 300 N.

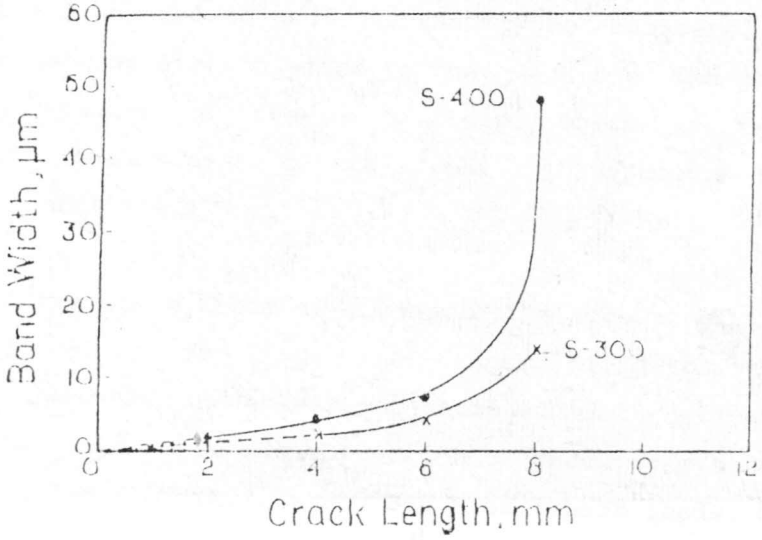

Fig. 8: Comparison between the discontinuous crack band size during cyclic shock loading at 300 N (S—300) and at 400 N (S—400) as a function of crack length.

larger as the crack is extended into the specimen. Cracks propagating under 300 N and 400 N of shock loading display comparable band width behavior (Fig. 8). Rough account of the band evolution indicates that their number matches the number of cycles spent on crack propagation in both fatigue and impact cases. Therefore, one may assume that each loading cycle caused a crack extension whose magnitude became progressively larger as the crack grew deeper.

The above explains how a very fast rate of loading may instigate stable crack growth in a brittle material. Microscopic processes at the crack tip in the form of crazing cause the elastic energy imposed by the dynamic load to yield qusiequilibrial crack growth. Note, however, that crack advance on the local level remains dynamic in nature. That is; the crack front advances through the preformed craze at once every single cycle then becomes arrested as it generates another craze. This coupled process is repeated every cycle within the duration of subcritical crack propagation. In this regard, the phenomenon at hand maintains a dual character. It is dynamic on the microscopic level and is quasistatic on the continuum scale. Accordingly, concepts of fracture mechanics could be employed to analyze the crack propagation behavior. In view of the fact that the observed crack propagation is quasiequilibrial, we correlate its rate to the static stress intensity factor.

Fracture Mechanics

Fracture mechanics theory provides an effective means to interrelate the material's resistance to crack propagation to the applied load and the configuration of the structure. On the other hand, fracture mechanics parameters could be used to guide the development of

materials with improved resistance to crack propagation. Methodically, the resistance to crack propagation addresses two fundamental questions. One is how strong ? The other is how long ?

The resistance of a material to crack propagation is commonly parameterized by the critical stress intensity factor K_{IC} [9] or the critical energy release rate J_{1c}[10]. The two parameters represent a strength measure for the resistance to the onset of crack propagation. The first implies that the material is linearly elastic. The latter theorizes that the material is elastoplastic, i.e., crack tip plasticity contributes to the resistance to crack growth. In general, $J_{1c} * G_{1c} = K^2_{1c}/E$, where E is the elastic modulus.

The question of how long, on the other hand, is considered by various laws relating the rate of crack propagation to the stress intensity factor, K_1 which is in turn related to the energy release rate in the manner show above. The most common crack propagation law is that of Paris, i.e.,

$$da/dN = A\ (\Delta K)^n \qquad (1)$$

where da/dn is the rate of crack propagation, N being the number of cycles, A and n are empirical parameters and K is the stress intensity range.

Our test operates at a zero minimum stress, hence the (maximum) stress intensity factor K_1 replaces the stress intensity range in Paris equation. For our test specimen (see Fig. 3) K_1 is given by [11]:

$$K_1 = \sigma\ (\pi\ a)^{\frac{1}{2}}.\ f(a/B) \qquad (2)$$

where is the stress, a is the crack length and B is the width of the specimen. The stress is given by:

$$\sigma = 6M/B^2 \qquad (3)$$

where M is the bending moment over the specimen width B. The geometric function f(a/B) is expressed as [11]:

$$f(a/B)=1.122-1.40(a/B)+7.33(a/B)^2-13.08(a/B)^3+14.0(a/B)^4$$

Data Analysis

Logarithmic plots of the average crack speed as a function of the maximum stress intensity factor are shown in Figs. 9 and 10. Each of the curves exhibits the conventional S-shaped character. An initially sharp rise in the crack speed (Stage I) is followed by a region of reduced acceleration (Stage II) at the end of which the speed rises suddenly (Stage III) towards ultimate failure. The linearity implied by Paris equation is obviously violated.

Figure 9 compares the crack propagation behavior under comparable impact and fatigue loads of 300 N. At 340 N, the same disparity between fatigue and cyclic shock persists as illustrated in Fig. 10. Above this load level (340 N) fatigue fracture occurs instantaneously. The data demonstrates a consequential difference in the crack propagation behavior under cyclic impact and conventional fatigue loading. The same material is more resistant ro crack propagation under repeated shock loading than under cyclic fatigue.

Figure 11 compares the crack propagation kinetics under various levels

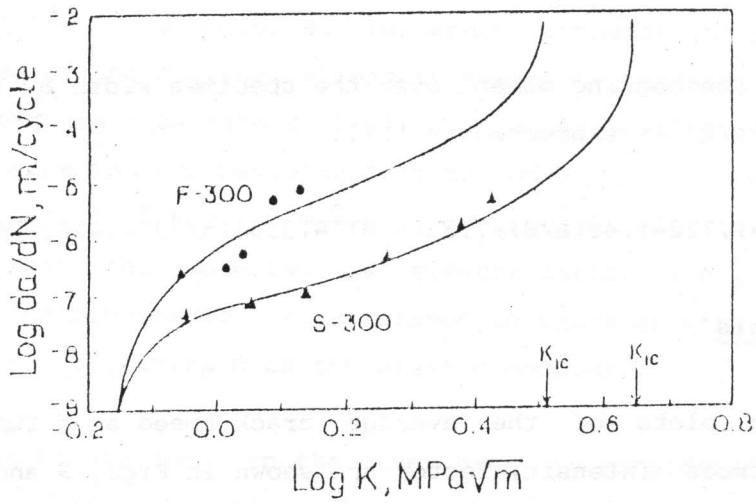

Fig. 9: Logarithmic plots of the rate of crack propagation for cyclic shock (S—300) and fatigue (F—300) as a function of the stress intensity factor. The critical stress intensity factors are marked by the downward arrows.

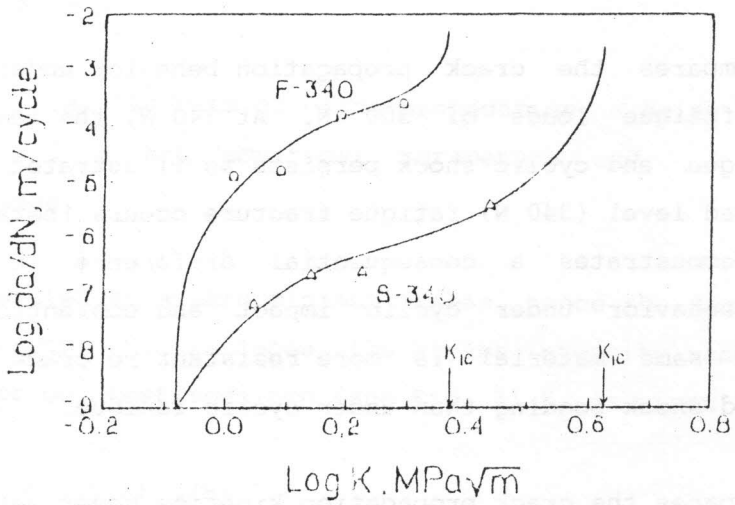

Fig. 10: Logarithmic plots of the rate of crack propagation for cyclic shock (S—340) and fatigue (F—340) as a function of the stress intensity factor. The critical stress intensity factors are marked by the downward arrows.

of cyclic shock loads. The S-shaped pattern in again displayed. Note, however, that the influence that the maximum shock load exerts on the crack kinetics does not appear to be monotonic. Within acceptable experimental variance, the crack kinetics is similar under 300 N and 340 N of maximum shock. Nevertheless, a significant difference is noted between these and the crack behavior under 370 N.

The actual critical crack length was measured from microscopic observations similar to that displayed in Fig. 5. From this information the critical stress intensity factor K_{1C} was calculated. Downward arrows in Figs. (9-11) indicate the respective K_{IC} values. Obviously, K_{1C} which is promoted as a material constant is far from being so. A plot of K_{1C} for the five testing conditions (Fig. 12) clearly emphasizes the strong dependence of K_{1C} on the loading condition. It is also noted that all the values reported exceed the known fracture toughness of PMMA (K_{1C} — 1 MPa.$m^{\frac{1}{2}}$). Moreover, cracks propagating under 300 N and 340 N of cyclic shock give rise to a fracture toughness value of about 4.5 MPa.$m^{\frac{1}{2}}$ which well exceeds that observed under a variety of single impact loading conditions [4]. This lends further support to the contention that a single strike impact loading influences the material differently from cyclic shock. The data presented in Fig. 12, in addition, challenges the constancy of K_{1C}, particularly for polymeric materials such as PMMA.

The nonlinear crack propagation behavior and the incongruity between fatigue and repeated shock resistance cannot be explained by crack propagation laws founded on linear elastic fracture mechanics such as Paris equation. Recent analyses of fatigue crack propagation in PMMA [12,13] reach a similar conclusion. It appears that the evolution of the craze zone ahead of the crack tip controls the rate of crack

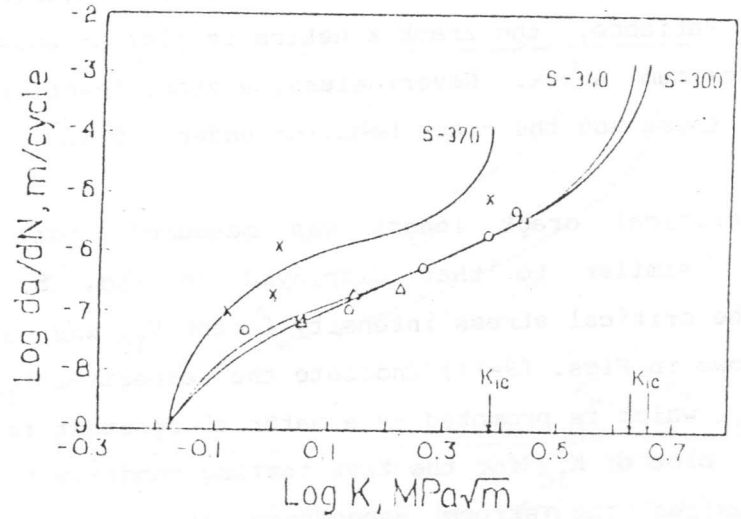

Fig. 11: Logarithmic plots of the rate of crack propagation under different cyclic shock loads as a function of the stress intensity factor. The arrows point out to the critical stress intensity factors.

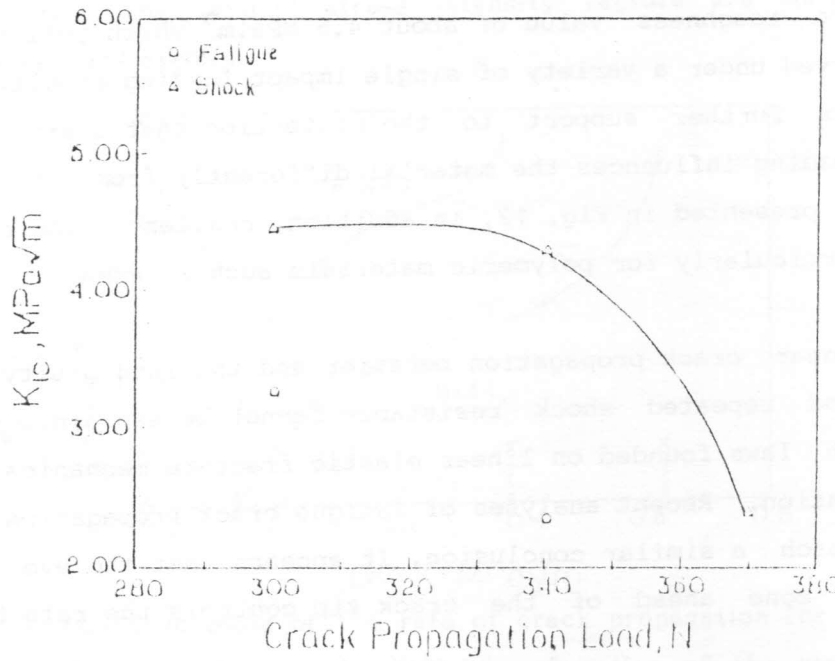

Fig. 12: Dependency of K_{IC} on loading conditions.

propagation. The Crack Layer theory [14] provides a rational explanation for the observed phenomena. The theory has been recently employed to analyze fatigue crack propagation in PMMA [13] and crack tip damage evolution in Epoxy resin [15] which as more brittle than PMMA.

The Crack Layer theory derives the rate of crack propagation as:

$$\frac{da}{dN} = \frac{\beta \, J1 \, \langle b \rangle}{\gamma^{*} R_1 - J_1} \qquad (5)$$

The numerator of the right hand side of Eq. (5) expresses what the theory defines as the rate of energy (irreversible work) expended on submicroscopic processes within the active (craze) zone leading to damage generation. It is related to the energy release rate J_1 and the average active zone size <b> through a phenomenological coefficient whose dimension is S^{-1}. The denominator expresses the crack driving force as the difference between the energy release rate J_1 and the energy required for crack advance $\gamma^{*} R_1$. The latter is the volume of damaged material within the active ("plastic") zone per unit crack extension R_1 multiplied by the specific enthalpy of damage γ^{*}. The latter is a material constant characteristic of its resistance to crack propagation.

The above rationale may be invoked to explain the two major issues raised by the present study; that is, the nonlinear crack propagation behavior and the higher resistance of the material to crack propagation under cyclic impact.

The rate or crack propagation is proportional to the rate of energy

4. Conclusions

(1) An experimental technique to test the material resistance to crack propagation under cyclic impact loading is presented. The equipment has been designed on basis of the Hopkinson's bar technique. The same equipment can be also used to study fatigue crack propagation.

(2) Tests conducted on PMMA revealed that the material is more resistant to crack propagation under cyclic impact than under fatigue.

(3) Fractographic evidence suggests that the crack under both loading conditions propagates in a discontinuous fashion. Quantitative analysis of the discontinuous crack propagation bands indicates that the crack jumps through a preceding craze once per cycle.

(4) Plots of the crack propagation rate as a function of the stress intensity factor display significant nonlinearity. This behavior was explained on basis of the Crack layer theory.

References

[1] S.P. Shab "A Model to Predict Fracture of Concrete Subjected to Varying Strain Rate", In "Dynamic Constitutive Failure/Models", A.M. Rajendran and T. Nicholas (Eds., AFWAL-TR-88/4229, December (1988).

[2] E. Plati and J.G. Williams, "The Determination of Fracture Parameters for Polymers in Impact", Polym. Eng. Sci., 15 pp. 470 -477 (1975).

[3] G.C. Adams and T.K. Wu, "Material Characterization by Instrumented Impact Testing", in Fallure of Plastics, W. Brostow and R.D. Coreliussen (Eds), Hanser Publishers, New York, pp. 144-168 (1986).

[4] S. Sahraoul, "Effects Dynamiques dans less Essais de Rupture aux Grandes Vitesse de Chargements. Etude de Quelques Polymers", Ph.D. Thesis, The University of Bordeaux I, France (1986).

[5] H. Kolsky, "An Investigation of the Mechanical Properties of Materials at Very High Rates of Loading", in "Dynamic

Constitutive Fallure/Models", A.M. Rajendran and T. Nicholas (Eds.), AFWAL-TR-88/4229. December (1988).

[6] E.M. Badawy, A.I. Gomaa, A.H. Hamdy and H.A. Elkadi, "An Experimental Apparatus to Produce Impact Fatigue Load", Bull. Faculty of Eng., Alexandria University, vol. xxiv. pp. 779-800 (1985).

[7] R.L. Slerakowski, "High Strain Testing of Composites", in Dynamic Constitutive Failure/Models", A.M. Rajendran and T. Nicholas (Eds.), AFWAL-TR-88/4229, December (1988).

[8] W. Doll and G.W. Weidman, "Transition from Slow to Fast Crack Propagation in PMMA", J. Mater Sci.-Letters, 15, pp. 2348-2350 (1976).

[9] ASTM Standard E399-78A, Annual Book of ASTM Standards, Part 10, p. 540 (1979).

[10] ASTM Standard E813-81, Annual Book of ASTM Standards, Part 10, p. 882 (1979).

[11] H. Tada and G.R. Paris, "The Stress Analysis of Cracks-Hand Book", Del Researcg Corp., St, Louis, Missouri (1985).

[12] E.P. Tam and G.C. Martin, "Fatigue Models for Glassy Polymers", J. Macromol. Sci,-Pys., B23, pp. 415-433 (1985).

[13] L. Koenczoel and K. Sehanobish, "Application of the Crack Layer Theory of Fatigue Crack Propagation in PMMA", J. Macromol.Sci,-Phys., B26, pp. 307-323 (1987).

[14] A. Chudnovsky and A. Moet, "Thermodynamics of Translational Crack Layer Propagation", J. Mater. Sci., 20, pp. 630-635 (1985).

[15] X. Wang, K. Sehanobish and A. Moet, Polymer Composites, 9, pp. 165-171 (1988).